

Sustainable Energy for An LED Lighting System Using Novel Control Algorithm for Constant Power Regulation

Dr. P. Soundar Rajan ^{1*}, Dr. Rajkumar Kupppapillai ², Dr. M. Arul Prasanna ³,
Dr. Kevin ARK Kumar ⁴

¹ Department of Electrical and Electronics Engineering, Jai Shriram Engineering College,
Tirupur, Tamil Nadu

² Department of Electrical and Electronics Engineering, Saranathan Engineering College, Trichy,
Tamil Nadu.

³ Department of Electrical and Electronics Engineering, PSNA College of Engineering and Technology,
Dindigul, Tamil Nadu.

⁴ Materials Management, High Pressure Boiler Plant, Bharat Heavy Electricals Limited, Trichy

*Corresponding author E-mail: soundarrajanpsr@gmail.com

Received: July 18, 2025, Accepted: August 25, 2025, Published: September 14, 2025

Abstract

A solar photovoltaic-driven interior LED lighting system is proposed in this manuscript, which is applicable for clean rooms, laboratories, modular offices, convention halls, theatres, churches, etc., during daytime as well as night hours. The proposed scheme gets supply from the grid in the case of shortage/absence of solar PV power. The power transfer from the PV source and the grid is customized to utilize the maximum PV power to maintain the constant and required level of illumination at the workplace. A Firefly algorithm, together with a conventional proportional-integral (PI) controller, is designed and tested successfully for effective power arrangement. The simulated and measured result shows the effectiveness of the new approach.

Keywords: Solar Photovoltaic; LED Lighting; Firefly Algorithm; Dual-Input; MATLAB/SIMULINK.

1. Introduction

The worldwide increase in energy demand under recent environmental issues related to power generation, has sparked much interest in the location of renewable energy sources. Generating solar power has become increasingly important for the world environment for the essential use of global resources. Trapping solar energy to light the Light Emitting Diode (LED) is one of the new developments in technology. An eco-friendly (LED) light system for sustainable living has been developed in recent years, which traps the solar energy from the sun. The battery bank in the conventional PV lighting system is charged through the converter and delivers the power through the converter module to the LEDs. Most types of DC lighting systems are used in street lights, E-vehicles, and Traffic signals, and are rarely used for domestic and biomedical purposes, etc. [1-4]. The combination of PV panels with high-power LEDs makes a new green lighting technology that can work at very high efficiency. The popular methods of driving LED arrays are constant voltage control, constant current control, and constant power control [5-11]. The above-mentioned methods have certain advantages and disadvantages that depend on the different types of applications.

Recently, the concept of solar light to interior light systems has been introduced in [12], [13], where the PV directly feeds the LED lighting system through a DC-DC converter. This finds application in photo-catalytic reactors of water treatment plants, traffic signals, illuminated display boards, etc. The work reported in [12] employs a PV system and two cascaded DC-DC converters directly feeding the LED lighting system. The first converter is employed for maximum power point tracking (MPPT) of the PV array, and the second converter is employed for driving the LED array. The applications mentioned in [12] demand maximum power point tracking as a prerequisite, and hence, the MPPT function is permanently enabled; in other words, the output power regulation is redundant.

The concept of the present work stems from the fundamental concept available in [12] with necessary modifications and improvements. This paper proposes an indoor lighting scheme for air-conditioned halls, clean rooms, laboratories, modular offices, convention halls, cinema theatres, churches, etc., where a huge amount of artificial lights are used even during daytime. This scheme has several advantages over AC-powered lights, namely low conversion loss, high luminous efficiency, environmental friendliness, and utilization of renewable energy, leading to reduced electricity bills. The above-mentioned applications demand a constant illumination level in order to maintain the required comfort for the satisfactory functioning of the people. Since the variation in solar radiation and temperature plays a crucial role in PV output power, causing a change in LED illumination, output power regulation becomes mandatory during varying climatic conditions.

In order to provide constant LED illumination under varying climatic conditions, this work proposes an additional input DC source to the LED lighting system. The resulting scheme is labelled as a Dual input Light to Light (LtL) conversion system in this paper. This additional DC source can be either a battery or an AC/DC rectifier, depending on the economic feasibility and/ or availability. While several papers have been published about LED lighting schemes, the development of an input LED lighting scheme with the LtL concept is not seen in the available literature.

Though the PV power dual-input LED lighting system is reliable, it provides partial grid independence and maintains good power regulation. But the power flow control from PV and the grid is cumbersome. Maximum power point tracking (MPPT) and sustainable constant power, but the outputs are to be maintained simultaneously in the system; The power flow controller always regulates the power at the output and traps maximum power by the MPPT controller. When an LED receives a shortage of power from the PV, the DC source feeds necessary power to the LED when there is a shortage/absence of power from the PV. With surplus power from PV, the system has a single goal to maintain the desired regulated power. Classical MPPT techniques (Perturb-and-Observe, Incremental Conductance) are attractive for low-cost drivers but can dither around the maximum power point, degrade under fast irradiance ramps, or stall in multi-peak conditions caused by partial shading. Rule-based supervisory loops for dual-input systems add robustness yet still face the exploration-exploitation trade-off between quick tracking and power ripple.

Bio-inspired metaheuristics algorithms such as Genetic Algorithms (GA), Particle Swarm Optimization (PSO), and the Firefly Algorithm (FA) were introduced to improve global search under nonconvex PV characteristics and to coordinate multi-objective goals (maximize PV harvest while enforcing output-power regulation). Among these, PSO models particles that share a global best and personal best, often converging rapidly but sometimes prematurely, especially when power surfaces are flat or noisy. Firefly Algorithm, in contrast, modulates agent attraction by perceived “brightness” (fitness) and distance with a randomization term that naturally balances local intensification and global diversification; its attractiveness decay with distance helps FA escape local plateaus while still clustering around promising regions. In practice this can translate to shorter effective settling and reduced output-power turbulence during set-point acquisition compared to PSO or GA under partial shading and load steps, provided FA parameters (α , β_0 , γ) are tuned to the converter dynamics and sampling rate (Yang, 2009). In the proposed dual input LtL system, the buck boost converter feeds LED with PV array and DC source. The power switches are controlled by the closed-loop control system by varying the duty ratio. The modulation of the duty ratio of the series switch connected to the PV system is adjusted by the Firefly algorithm (FA), whereas the second switch connected to the DC source is controlled through a traditional proportional-integral (PI) controller. For a dual-input LtL system, the broad goal is constant LED power (illumination), while the inner goal is to maximize the PV contribution subject to that constraint. FA’s distance-weighted attraction is well-suited to this bilevel objective. FA’s stochastic search creates brief, decaying excursions around the optimum duty for the PV switch before settling, which is observed experimentally as short-lived “turbulations” followed by a quick lock to the target power. This minimizes visible flicker and electrical stress. When shading abruptly reduces PV capability, the FA loop saturates at the PV limit and a secondary PI loop on the auxiliary-source switch backfills the deficit—yielding degradation with rapid recovery when irradiance returns. In embedded MPPT, where only a handful of samples per electrical time constant are practical, FA maintains exploration without excessive overshoot. Overall, FA offers a favorable speed-ripple-robustness trade-off for constant-power LED regulation in dual-input PV systems, especially under partial shading and set-point steps, while remaining lightweight enough for microcontroller implementation. The reason for FA to be employed for PV output power regulation lies in its capability of faster convergence and minimum duration of PV output power fluctuations during power tracking [13], [14]. The firefly algorithm (FA) is employed in the PV system to change the duty ratio. The closed-loop control scheme is controlled with the microcontroller, and the performance of the control strategy is validated through simulation as well as field studies at various atmospheric conditions.

2. Methods and Materials

The power circuit of a dual-input LT conversion system is shown in Fig.1. Here, there are two voltage sources V_{pv} and V_b , the suffixes denote PV array and DC source, respectively. The equivalent circuits of each mode are given in Fig. 3(a), 3(b), and 3(c). Modes 2 and 4 are the same except for the initial values. The controlled main switches S1 and S2 are identified as MOSFETs, and two freewheeling diodes are named as D1 and D2 to control the current from the PV source V_{ph} to the DC source V_b . When S1 is switched ON, the inductor at the output L and filter C are selected for continuous current flow.

Referring to the circuit in Fig.1, at any time the status of switches is given below:

- 1) S1 conducts
- 2) S2 conducts
- 3) Both S1 and S2 are OFF

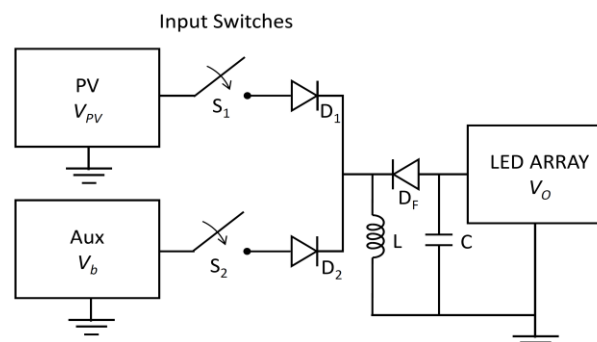


Fig. 1: Dual-Input LtL Converter LED Lighting Scheme.

Accordingly, there are four modes of operation, and in each mode of operation, the inductor current i_L and capacitor voltage v_c are considered as the two state variables to derive the state space models. The steady state waveforms of inductor voltage and current for one cycle are depicted in Fig. 2. Here, the four modes of operation exist during the total time period, T . During mode 1, the switch S_1 is closed for d_1T seconds, and during mode 3, switch S_2 is closed for d_2T seconds. Modes 2 and 4 are made equal where both S_1 and S_2 are OFF, and the diode DF alone conducts.

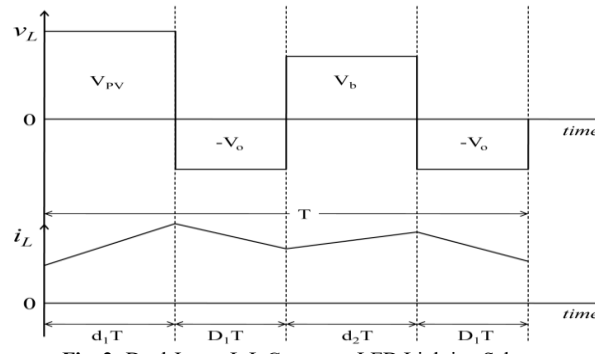


Fig. 2: Dual-Input LtL Converter LED Lighting Scheme.

The circuit operation in each mode is vividly considered, and differential equations for each mode are derived. Let x_1 and x_2 denote state variables, then $x_1 = i_L$ and $x_2 = v_c$. The equivalent circuits of each mode are given in Fig. 3.

Mode 1 - ($0 < t < d_1T$)

Mode 2 - ($d_1T < t < D_1T$)

Mode 3 - ($(d_1T + D_1T) < t < (d_1T + D_1T + d_2T)$)

Mode 4 - ($d_2T < t < D_2T$)

Employing the state-space averaging technique [15], transfer functions of the dual-input buck-boost converter for the LED lighting scheme can be obtained by the following equation:

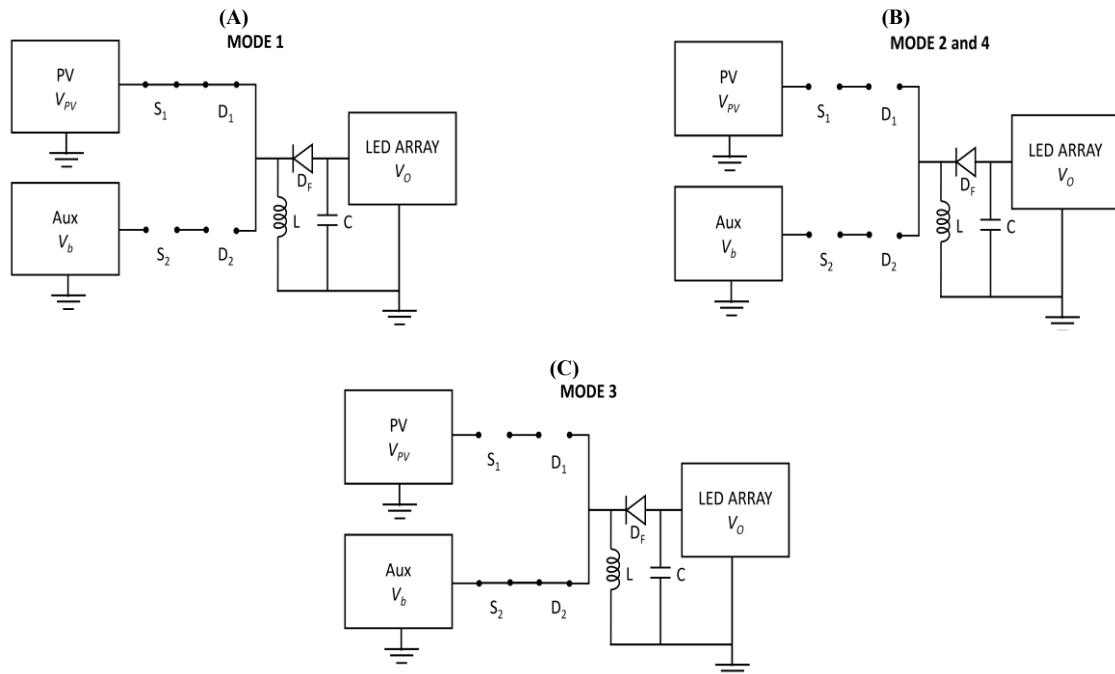


Fig. 3: Modes of Operation. (A) Mode 1, (B) Modes 2 and 4, (C) Mode 3.

$$\frac{V_o}{d_2} = \frac{r's^2 + \left[r'n + d'rh - \frac{r'^2}{Cr_c^2} \right] s + \left[d \left(\frac{hr'}{C(R+r_c)} + \frac{h'r'^2}{r_c^2} \right) - \frac{r'r_c}{LC} \left(r'_L + d'r' \left(\frac{R-d'}{R+r_c} \right) \right) - rx_1m \right]}{s^2 + ns + m} \quad (1)$$

Where

$$d' = 1 - d_1 - d_2 \quad (2)$$

$$r' = \frac{Rr_c}{(R+r_c)} \quad (3)$$

$$m = \frac{r_L(r_c + R) + d'Rr_Lr_c}{LC(R+r_c)^2} + \frac{dR}{r_c(R+r_c)^2} \quad (4)$$

$$n = r_L + d'r' + \frac{1}{C(R+r_c)} \quad (5)$$

$$h = r' \frac{x_1}{L} + \frac{x_2}{L(R + r_c)} + \frac{v_{pv}}{L} \quad (6)$$

The closed-loop scheme of the system is shown in Fig. 4. The dual-input buck-boost converter (DIBBC) represents the transfer function presented in (1). For the specifications given in Appendix A of the DC-DC converter, the pole placement technique [16] is employed to compute the PI controller constants, and the proportionality constant K_p is found as 0.6946, and the integral constant K_i as 4.54.

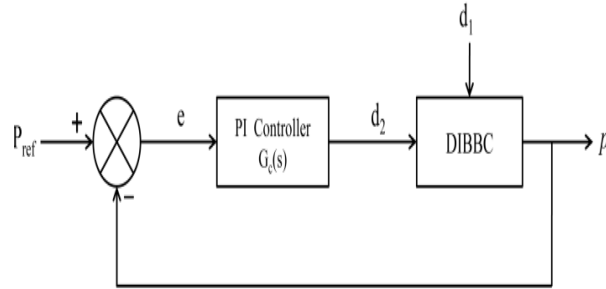


Fig. 4: Control Scheme of the System.

The block diagram of the setup is shown in Fig. 5. The power management is achieved with the help of a biologically inspired optimization method, namely the firefly algorithm (FA) and the traditionally designed proportional-integral (PI) controller. The FA is employed for power flow control from the PV array, while the PI controller adjusts the duty ratio of switch S_2 , in case of a deficiency in the PV power.

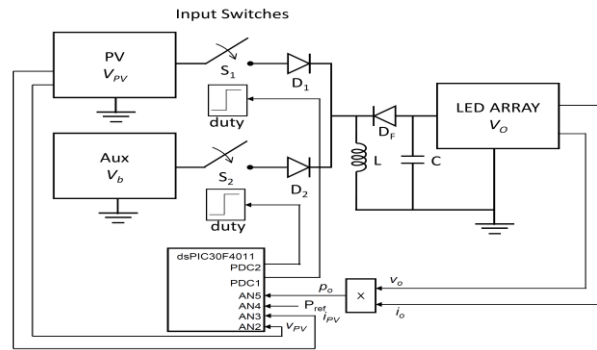


Fig. 5: Experimental Setup.

In the above control scheme, the power at the output is continuously maintained and sensed by the controller with respect to the change in set value. The Firefly Algorithm (FA) is employed in the controller for the power control. If the load power exceeds the maximum Power Point (MPP) of the PV array, the controlled switches S_2 are switched on to trap the remaining power from the DC source. The control strategy is to sense P_o , adjust the duty ratio of switch S_1 through the Firefly algorithm, and stop changing the variation in the duty ratio of switch S_1 when $P_o = P_{ref}$ or MPP is reached, whichever comes first. If MPP has already been reached and when $P_o < P_{ref}$, the duty ratio of switch S_2 is varied by using a PI controller. The flowchart for the firefly algorithm for power flow is shown in Figure 6.

3. Results and Discussions

A 12W prototype DC-DC converter with an LED lighting scheme was made up in the laboratory, and results were obtained at the different operating points, and The obtained results are shown in the figure. This figure illustrates the dynamic performance of the proposed dual-input LtL system under two disturbance scenarios: (i) a step change in the LED power reference and (ii) a sudden irradiance drop due to partial shading. In both cases, the system achieves convergence to the desired operating point with settling times of approximately 2.5 s (reference change) and 2.6 s (shading removal).

The short settling interval has important practical implications. In indoor lighting applications, illumination fluctuations persisting beyond 3 to 4 seconds are often perceptible to occupants as flicker or discomfort, particularly in task-lighting environments. By maintaining recovery less than 3 seconds, the proposed FA-based controller ensures that such transients remain below the threshold of visual disturbance, thereby upholding visual comfort standards. In outdoor LED systems, faster stabilization also translates into tighter illuminance regulation, which is critical for energy efficiency and uniformity.

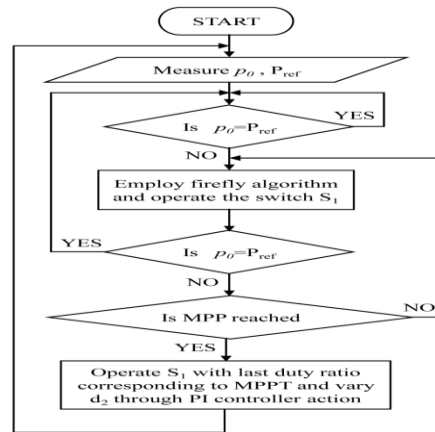


Fig. 6: Flow Chart of Output Power Regulation.

Power fluctuations observed during the transient phase are brief and decay rapidly, a signature of the FA's exploratory search behavior. Rather than causing sustained oscillations, these "turbulations" facilitate global search before convergence, resulting in smooth steady-state operation without long-term ripple. From a reliability standpoint, this mitigates thermal and electrical stress on both the PV array and LED driver, extending component lifetime compared to methods that induce continuous oscillation around the set-point (e.g., Perturb-and-Observe).

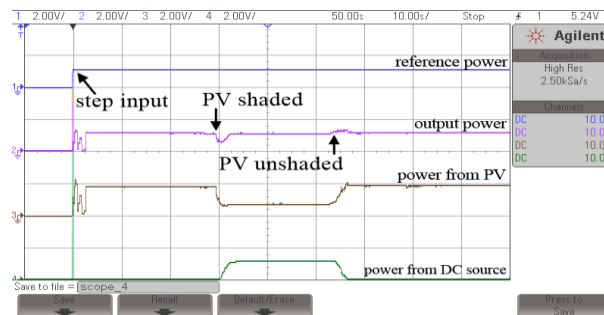


Fig. 7: Experimental Results.

When compared to existing MPPT and LED regulation schemes, the superiority of the proposed system becomes clear. Conventional Perturb-and-Observe or Incremental Conductance techniques typically exhibit longer settling times ($>4\text{--}5$ seconds) under partial shading, with steady-state oscillations that can reduce net energy capture. PSO, while faster in smooth irradiance profiles, has been reported to converge prematurely under multimodal PV curves, requiring re-initialization and leading to prolonged disturbances. In contrast, the FA-based strategy achieves consistent convergence (less than 3 seconds) across both reference and irradiance disturbances, with negligible steady-state error. Thus, the results in Fig. 7 substantiate that the proposed dual-input FA-controlled LtL system offers a superior speed–stability trade-off, delivering both rapid recovery and stable illuminance, making it well-suited for mission-critical lighting domains where both energy efficiency and user comfort are important. While FAs provide tangible advantages in robustness and tracking performance, a few limitations must also be acknowledged for PV-fed LED applications.

FA involves iterative fitness evaluation and distance-based attractiveness calculations across a population of fireflies. Although the per-iteration arithmetic is modest, the total overhead grows with swarm size and search dimension. In small-scale converters (≤ 50 W) driven by low-cost microcontrollers, careful tuning of the swarm size is necessary to ensure that execution fits within sampling deadlines without degrading control bandwidth. Also, poorly tuned parameters may lead to slow convergence or excessive oscillations. Regardless of the optimization method, field performance is influenced by real-world maintenance issues. PV modules accumulate dust and experience thermal cycling, reducing effective irradiance capture and potentially masking algorithmic gains. Similarly, LED junction degradation and driver aging can shift the optimum operating point over time. These factors necessitate regular cleaning, inspection, and recalibration, highlighting that control alone cannot substitute for operational maintenance.

By recognizing these limitations, researchers and practitioners can approach FA-based PV–LED control with a more balanced perspective: exploiting its superior dynamic performance and robustness under partial shading, while combining it with pragmatic considerations such as hybrid supervisory control, parameter adaptation, and scheduled maintenance for long-term viability.

Future research could focus on optimizing the Firefly Algorithm for faster convergence in larger multi-string PV–LED systems and exploring hybrid control architectures that combine FA with conventional PI or MPPT methods to reduce computational burden. Integration with smart grid technologies presents another opportunity, enabling dynamic power management, demand response, and improved grid interaction. Adaptive tuning of FA parameters through machine learning could further enhance robustness under variable irradiance and load conditions. In parallel, long-term studies are needed to quantify the economic and environmental benefits of reduced battery reliance, as well as the impact of FA-based control on system reliability, PV degradation, and LED driver lifespan.

4. Economic Analysis

The proposed lighting technology aims to provide illuminance to establishments during the day, consuming less energy at an affordable cost. For illuminating an office room with ten 12W LED fittings, the total installation cost will be around INR. 27,000. The breakup of prices of various components of the installation is shown in Fig. 8.

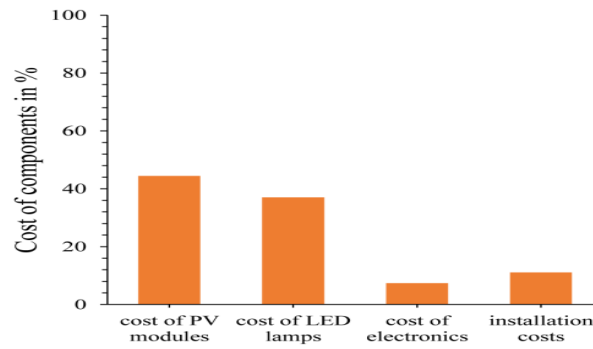


Fig. 8: Cost-Wise Breakup.

The lifetime of a solar PV panel is around 20 years, and the LED lamp will need to be replaced after 12 years. The general assumptions and variables of economic analysis are tabulated in Table 1.

Table 1: General Assumptions for Economic Analysis

Description	Values
Total power of the LED lamps	120 W
Average hours of operation per day	10 hrs
Battery capacity	100 Ah
Utility tariff	Rs. 8 / kWh
Battery replacement	Once in 4 years
1 Indian Rupee (INR)	0.016 USD

To obtain the economic analysis, the following systems were compared

- Case 1: Utility-powered LED lighting system
- Case 2: Combined solar PV and battery-powered LED lighting system
- Case 3: Combined solar and rectified utility source

In the normal LED Lighting system, the customer pays a monthly tariff based on usage, and a converter circuit is required to power the LED Lamps. In the off-grid PV system, the solar panels for the PV array and battery bank are selected based on the power consumption and autonomy. Here, the battery bank is replaced at certain time intervals, which may be 5 or 6 years, and disposal of the used battery bank raises certain environmental issues. The combined solar PV and DC source is employed with the bridge rectifier, with an appropriate filter for the rectification process from the utility AC source.

The energy from solar PV is assumed free of cost, as the operation and maintenance costs for smaller systems are almost negligible. In case 2, the initial cost may be higher, but the trapped energy is free of cost with negligible running cost for a smaller system. In cases 1 and case 3, the running and consumption costs based on the utility tariff system are calculated by instant power consumption $E_{AC(inst)}$ from the utility [19]. and multiplying it by the prevailing tariff charges as given below:

$$\text{Daily energy cost} = \left(\sum_{t=0}^{24} E_{AC,inst} \times t \right) \times \text{Tariff} \quad (7)$$

The economic comparisons between the three cases are illustrated for the period of ten years in Figure 9. The accumulated cost for the three cases is also given in Figure 9. The battery replacement costs are included at the end of the fourth and eighth years, respectively.

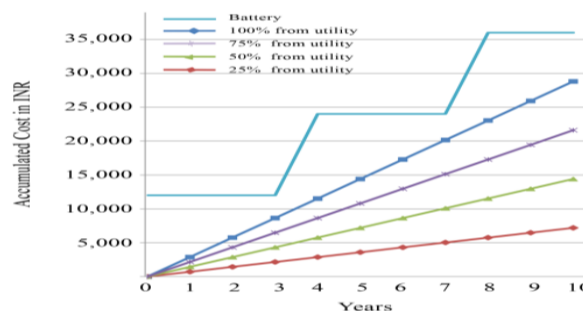


Fig. 9: Economic Comparisons of Different Cases.

The system mentioned in case 3 is again divided into three types, wherein 40% of power comes from the utility and the remaining 60% from the solar, and vice versa, or 50% from both solar and utility. The overall cost for the case 2 system exceeds the cases 1 and 3, but no additional installation and wiring charges are needed. The overall cost for the case 2 system exceeds that of cases 1 and 3, but no additional installation and wiring charges are needed.

In Case 2, the recurring cost of battery replacement becomes a dominant factor. Lithium-ion or lead-acid storage typically requires replacement every 4–6 years under daily cycling, meaning that over a 10–12-year horizon, at least two complete battery replacements would be necessary. Under the baseline energy use, even modest tariff escalation of 4 to 6% plus declining/credited battery costs (20–40%) typically reduces the breakeven inside a 10–12-year window, and after which Case 2 becomes strictly cheaper than utility-only because fuel (grid) costs compound while PV energy does not. Over 15–20 years, cumulative grid kWh avoided by Case 2 dominates the footprint of periodic battery swaps when recycling is enforced, whereas conventional cases accumulate operational emissions indefinitely. In short, conventional cases pay both financially and environmentally every year. Therefore, Solar PV with a DC source LED lighting scheme is an economically viable one.

5. Conclusion

This paper presents a novel dual-input Light-to-Light (LtL) system architecture, wherein the LED lighting load is powered directly by a photovoltaic (PV) array, thereby eliminating intermediate energy storage elements and enhancing overall system efficiency. To ensure consistent and reliable illumination irrespective of solar irradiance fluctuations, a stiff auxiliary source is integrated as a secondary input. The proposed system leverages a real-time power budgeting strategy and an adaptive control mechanism to optimally manage the energy flow between the PV source and the auxiliary input. The effectiveness of the design has been validated through both detailed simulation studies and experimental hardware implementation under dynamically varying atmospheric conditions. Furthermore, a comprehensive analysis of economic viability underscores the practical relevance of the system for sustainable lighting in both grid-connected and remote applications. The results affirm that this dual-input LtL approach offers a promising and cost-effective solution for modern energy-efficient lighting infrastructure.

6. Appendix

Table 2: Hardware Details

Hardware Specification	Value
Switching frequency	40kHz
Inductance, L	1.813mH
Internal resistance of inductor, rL	0.5Ω
Capacitance, C	470μF
Internal resistance of capacitor, rC	0.01Ω

References

- [1] PLTU PT Puncakjaya Power Team, "Analysis of the utilization of LED lighting systems using solar panels," *All Studies J.*, vol. 9, no. 5, 2024.
- [2] H. Tian, X. Zhou, and J. Zhang, "Tri-port DC–DC buck–boost converter for photovoltaic LED drivers," *Energy Reports*, vol. 9, pp. 1660–1674, 2023.
- [3] M. Li, R. Zhang, and F. Qian, "Hybrid solar-fiber and PV system for daylight and electrical lighting via spectral splitting," *Appl. Energy*, vol. 322, 2022, Art. no. 119387.
- [4] R. D. Orejon-Sanchez, J. R. Andres-Diaz, and A. Gago-Calderon, "Autonomous Photovoltaic LED Urban Street Lighting: Technical, Economic, and Social Viability Analysis Based on a Case Study," *Sustainability*, vol. 13, no. 11746, Oct. 2021. <https://doi.org/10.3390/su132111746>.
- [5] N. Femia and W. Zamboni, "Photovoltaic-fed LED lighting system with SOC-based dimmable LED load," in *IECON 2012 – 38th Annual Conference on IEEE Industrial Electronics Society*, Montreal, QC, pp. 1132–1137, 2012. <https://doi.org/10.1109/IECON.2012.6388613>.
- [6] B. R. Lin and C. L. Huang, "Analysis and implementation of an integrated sepic-forward converter for photovoltaic-based light-emitting diode lighting," *IET Power Electronics*, vol. 2, no. 6, pp. 635–645, Nov. 2009. <https://doi.org/10.1049/iet-pel.2008.0176>.
- [7] M. Ali, M. Orabi, E. Abdelkarim, J. A. A. Qahouq and A. E. Aroudi, "Design and development of energy-free solar street LED light system," in *IEEE PES Conference on Innovative Smart Grid Technologies - Middle East*, Jeddah, pp. 1–7, 2011. <https://doi.org/10.1109/ISGT-MidEast.2011.6220812>.
- [8] J. Hernandez, J. Silva and W. Vallejo, "Study of implementation of PV-powered LED system to be used as traffic lights in the Bogota city," in *37th IEEE Photovoltaic Specialists Conference*, Seattle, WA, pp. 003250–003253, 2011. <https://doi.org/10.1109/PVSC.2011.6186631>.
- [9] Steve Winder, *Power Supplies for LED driving*, Elsevier Inc., 2008. <https://doi.org/10.1016/B978-0-7506-8341-8.00003-7>.
- [10] P. D. Teodosescu, M. Bojan and R. Marschalko, "Resonant LED driver with inherent constant current and power factor correction," in *Electronics Letters*, vol. 50, no. 15, pp. 1086–1088, July 17, 2014. <https://doi.org/10.1049/el.2014.1701>.
- [11] Q. Luo, S. Zhi, C. Zou, W. Lu and L. Zhou, "An LED Driver With Dynamic High-Frequency Sinusoidal Bus Voltage Regulation for Multistring Applications," *IEEE Trans. on Power Electronics*, vol. 29, no. 1, pp. 491–500, Jan. 2014. <https://doi.org/10.1109/TPEL.2013.2253335>.
- [12] Q. Luo, S. Zhi, C. Zou, B. Zhao and L. Zhou, "Analysis and design of a multi-channel constant current light-emitting diode driver based on high-frequency AC bus," *IET Power Electronics*, vol. 6, no. 9, pp. 1803–1811, November 2013. <https://doi.org/10.1049/iet-pel.2012.0696>.
- [13] M. R. Amini, A. Emrani, E. Adib and H. Farzanehfard, "Single soft switched isolated converter with constant output current for light emitting diode driver," *IET Power Electronics*, vol. 7, no. 12, pp. 3110–3115, 12 2014. <https://doi.org/10.1049/iet-pel.2013.0281>.
- [14] Y. Hu and M. M. Jovanovic, "LED Driver With Self-Adaptive Drive Voltage," *IEEE Trans. on Power Electronics*, vol. 23, no. 6, pp. 3116–3125, Nov. 2008. <https://doi.org/10.1109/TPEL.2008.2004558>.
- [15] B. J. Huang, C. W. Chen, P. C. Hsu, W. M. Tseng, and M. S. Wu, "Direct DC sources-driven solar LED lighting using constant-power control," *Solar Energy*, 86, pp. 3250–3259, 2012. <https://doi.org/10.1016/j.solener.2012.07.028>.
- [16] N. Femia, M. Fortunato and M. Vitelli, "Light-to-Light: PV-Fed LED Lighting Systems," *IEEE Trans. on Power Electronics*, vol. 28, no. 8, pp. 4063–4073, 2013. <https://doi.org/10.1109/TPEL.2012.2229297>.
- [17] K. Sundareswaran, Kevin Ark Kumar, P.R. Venkateswaran, and S. Palani, "Solar photovoltaic fed dual input LED lighting system with constant illumination control," *Frontiers in Energy*, vol.10, issue.4, 2016, pp.473–478. <https://doi.org/10.1007/s11708-016-0420-z>.
- [18] T. Surinkaew and I. Ngamroo, "Coordinated Robust Control of DFIG Wind Turbine and PSS for Stabilization of Power Oscillations Considering System Uncertainties," *IEEE Trans. on Sustainable Energy*, vol. 5, no. 3, pp. 823–833, 2014. <https://doi.org/10.1109/TSTE.2014.2308358>.
- [19] K. Sundareswaran, S. Peddapati and S. Palani, "MPPT of PV Systems Under Partial Shaded Conditions Through a Colony of Flashing Fireflies," *IEEE Trans. on Energy Conversion*, vol. 29, no. 2, pp. 463–472, 2014. <https://doi.org/10.1109/TEC.2014.2298237>.
- [20] Davoudi and J. Jatskevich, "Parasitics Realization in State-Space Average-Value Modeling of PWM DC–DC Converters Using an Equal Area Method," *IEEE Transactions on Circuits and Systems I: Regular Papers*, vol. 54, no. 9, pp. 1960–1967, 2007. <https://doi.org/10.1109/TCSI.2007.904686>.
- [21] Benjamin C.Kuo, *Automatic Control System*, Eighth ed., Wiley-India, 2003.
- [22] Kevin Ark Kumar, K.Sundareswaran, and P.R.Venkateswaran, "Performance study on a grid connected 20kWp solar photovoltaic installation in an industry in Tiruchirappalli (India)," *Energy for Sustainable Development*, vol. 23, pp.294–304, 2014. <https://doi.org/10.1016/j.esd.2014.10.002>.
- [23] H. Mohsenian-Rad, V. W. S. Wong, J. Jatskevich, R. Schober and A. Leon-Garcia, "Autonomous Demand-Side Management Based on Game-Theoretic Energy Consumption Scheduling for the Future Smart Grid," *IEEE Trans. on Smart Grid*, vol. 1, no. 3, pp. 320–331, 2010. <https://doi.org/10.1109/TSG.2010.2089069>.
- [24] P. Soundar Rajan , M. Arul Prasanna , M. Nishar Ahamed , R. Sathish Kumar "Enhancing the performance and economic efficiency of range-extended electric vehicles: A hybrid dual stream spectrum deconvolution neural network with Beluga Whale Optimization" *Journal of Energy Storage* 104 (2024) 114450. <https://doi.org/10.1016/j.est.2024.114450>.